Piezotronic effect on the luminescence of quantum dots for micro/nano-newton force measurement

Yan Zhang[1,2], Jiaheng Nie[1], and Lijie Li[3](✉)

[1] School of Physical Electronics, University of Electronic Science and Technology of China, Chengdu, 610054, China
[2] Beijing Institute of Nanoenergy and Nanosystems, Chinese Academy of Sciences; National Center for Nanoscience and Technology (NCNST), Beijing, 100083, China
[3] Multidisciplinary Nanotechnology Centre, College of Engineering, Swansea University, Swansea, SA1 8EN, UK

ABSTRACT

The luminescence of semiconductor quantum dot (QD) can be adjusted by piezotronic effect. An external mechanical force applied on the QD generates piezoelectric potential, which alters the luminescence of the QD. A small mechanical force may induce significant change on the emission spectrum. For InN QD case, it is demonstrated that the un-forced emission wavelength is more than doubled by a 1 μN force. The strategy of using piezotronic effect to tune the colour of the emission leads to promising noncontact force measurement applications in biological, medical sensors and force sensitive displays. More piezoelectric semiconductor materials have been investigated in terms of the tuneability of the emission wavelength in the presence of an external applied force. It is found that CdS and CdSe demonstrate much higher tuneability $\delta\lambda/\delta F$, which will lead to micro/nano-newton force measurement applications.

Introduction

Nanometre sized semiconductor QDs have been found particularly promising in fluorescence biomarkers [1]. These nanoparticles can be attached with biosamples for both in vitro and in vivo studies. Since the first demonstration of using QDs in biological field, QDs have been successfully applied in various systems including fixed cell labelling, imaging of living cell dynamics, in situ tissue profiling, fluorescence detection, sensing and in vivo animal imaging [2] [3] [4] [5]. The main advantage of utilizing QDs for the biological sensing is the wavelength tuneability. It was reported that the emission wavelength of a QD can be adjusted by several factors including mechanical strain and internal piezoelectric field [6] [7]. The mechanism of external strain induced bandgap change can shift the emission wavelength, but normally a relatively large strain is required to have a profound bandgap changing [8] [9] [10]. Internal piezoelectric potential can effectively tilt the energy structure of the QD causing a redshift known as the quantum confined Stark effect (QCSE). Studies of the piezoelectric induced QCSE on semiconductor QDs were reported in [11] [12] [13] [14].

Address correspondence to L Li, email: l.li@swansea.ac.uk

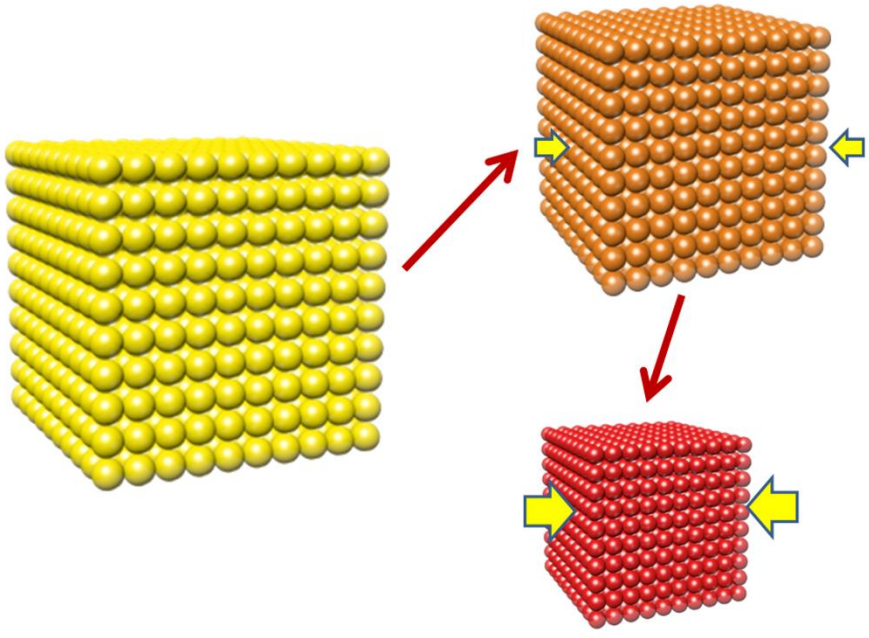

Figure 1, Schematic graph of QDs serving as deformation sensors. The piezoelectric semiconductor quantum dot is cuboidal.

QDs have been also extensively researched for display/light emitting applications [15] [16] [17] [18]. There have been several interesting exploitations in applying QDs in electromechanical systems including a method to detect the position of random distribution QDs in a solid photonic structure, where it was found that the emission frequency is highly sensitive to the mechanical stress [19]. Stress-induced performance change of the CdS nanocrystals has been reported in [20]. Semiconductor QDs have been embedded in electromechanical resonators in reference [21]. It was stated that the wavelength tuneability becomes a fundamental requirement for a number of new applications [22], which promotes the research and development in integrating QDs with electromechanical devices. Recent research concepts on piezotronic and piezophototronic [23] [24] [25] developed by Z. L. Wang has seamlessly connected the piezoelectric effect with micro- and nanoelectronics devices and systems, creating various new devices in areas of sensors and mechanical-to-electrical energy harvesting [26] [27] [28] [29] [30] [31]. In addition, piezoelectric effects on the luminescence of various materials systems were recently reported in [32] [33] [34]. The application of piezotronic into quantum dots offers a new cluster of adjustable/tuneable light emitting devices.

As the increasing interest of implementing QDs in biological sensing systems, it is stringent that a systematic investigation is conducted for the piezoelectric controllability on QDs made of various semiconductor materials. Figure 1 depicts a schematic graph of a cuboidal QD subjecting to external forces (shown in arrows). It is noted that this method is non-destructive and does not require any associated electronics. In this work, we study the wavelength tuneability of a range of quantum dots on the basis of the piezotronic effect with an example of the InN QD to demonstrate the method. Eight other materials are analysed in terms of the wavelength tuneability. The results reveal that some materials such as CdS can have much higher wavelength tuneability than other semiconductor materials.

Method

The effective energy EQD of semiconductor quantum dot considered bulk bandgap E_g, confined electron and hole energy E_e and E_h, excitonic binding energy E_{ex}, and piezoelectric potential E_p, which constitute the

$$E_{QD} = E_g + E_e + E_h - E_{ex} - E_p \quad (1)$$

E_e and E_h are attributed to the quantum confinement inducing the blue shift. Confined ground state energies can be expressed as $E_{e,h} = \frac{\hbar^2 \pi^2}{2m_{e,h} r^2}$, where $\hbar$ denotes the reduced Planck's constant, $m_{e,h}$ represent effective masses for electron and hole respectively, and r is the approximated radius. Exciton binding energy reduces the bandgap due to Coulombic attraction between electron-hole pair of the exciton. Due to the QCSE, strain induced piezoelectric potential ($F_e \bar{z}$) cause the electron states shifting to lower energies and hole states shifting to higher energies, leading to a redshift of luminescence. E_p can be calculated as the second order correction for the biased potential [35]

$$E_p = \frac{\left| \left\langle \varphi_2^{(0)} \left| eF_e z \right| \varphi_1^{(0)} \right\rangle \right|^2}{E_2^{(0)} - E_1^{(0)}} = 24 \left(\frac{2}{3\pi} \right)^6 \frac{e^2 {F_e}^2 m_{e,h} (2r)^4}{\hbar^2} \quad (2)$$

Mechanical strain of the QD generates piezoelectric potential that is governed by the piezoelectric equation

$S = s^E T + dE$

$D = dT + \varepsilon^T E$, where S, T, E, D represent strain, stress, electrical filed strength, and dielectric displacement respectively. s, d, ε denote mechanical compliance, piezoelectric constant and permittivity, where the superscripts to the symbols indicate the quantity kept constant under boundary conditions. Hence generated piezoelectric field subjecting to an external stress T is $F_e = \frac{dT}{\varepsilon_0 \varepsilon_r}$, and the piezoelectric charge $Q_p = dTA$, where A is the area of surface of the cube.

The excitonic emission may play a dominant role at a low temperature. At room temperature the electron thermal energy $k_B T$ normally exceeds the exciton binding energy, annihilating the excitons, subsequently reducing the luminescence intensity at the wavelength of excitonic emission. [36] Experimental results in reference [37] reported a significant enhancement of the luminescence by current injection for InGaN/GaN QDs. Apart from the ground energy bandgap that defines the energy/wavelength of the emitted photons, another important factor of the luminescence is the intensity, which is determined by the number of available free electrons. Piezoelectric effect generates space charges from the mechanical strain. As the emission process

is the inelastic electron-photon interaction, both the wavelength and intensity of the luminescence can be expressed by the quantum optics theory, which is [38]

$$R_{h-l} = \frac{2\pi}{\hbar}\left|M_{h-l}\right|^2 \rho_3^{op}(\hbar\omega) B(\hbar\omega) f_c(1-f_v) \quad (3)$$

Where R_{h-l} is designated as the transition rate of electrons moving from higher states in the conduction band to lower states in the valence band. $\left|M_{h-l}\right|^2$ is the squared matrix element coupling the higher and the lower states. $\left|M_{h-l}\right|^2$ is determined by the electron wavevector k and the polarization direction of the electromagnetic wave. In most III-V and II-VI semiconductors, the average value of the momentum matrix element can be treated as a constant. The density of photon states is expressed by $\rho_3^{op}(\hbar\omega) = \frac{(\hbar\omega)^2 n_r^2}{\pi^2\hbar^3 c^3}$. The Bose-Einstein occupation factor for photons is $B(\hbar\omega) = \frac{1}{e^{(\hbar\omega/k_B T)}-1}$. n_r represents the refractive index of the material, and c is the speed of light in vacuum. In the transition process, one needs to find the number of electrons in the conduction band, and vacant sites in the valence band, which can be mathematically defined by $f_c(1-f_v)$, where f_c and f_v stand for Fermi-Dirac distribution functions of electron states in the conduction and valence band respectively ($\frac{1}{e^{(E-\mu)/k_B T}+1}$). The total emission R_T for specific photon energy is the sum of all energy levels separated by this photon energy, that is

$$R_T = \sum_k R_{h-l}\delta(E_{hl} - \hbar\omega) \quad (4)$$

Delta function in the equation (4) defines the transition energy around the photon energy. In the equation (4), the sum of the Delta function with respect to k, $\int \frac{d^3k}{(2\pi)^3}\delta(E_{hl}-\hbar\omega)$, is essentially the density of states $\rho_3(E)$ in three-dimension for the bulk materials. In a bulk material, the DOS is

$$\rho_3(\hbar\omega) = \frac{1}{2\pi^2}\left(\frac{2m_r}{\hbar^2}\right)^{3/2}(\hbar\omega - E_g)^{1/2}$$
$$\hbar\omega \geq E_g \quad (5)$$

where E_g is the bandgap for bulk material. For the case of QD, as it is quantum mechanically confined in three dimensions, the 0D DOS is given by the Lorentzian equation

$$\rho_0(\hbar\omega) = \frac{2}{\pi}\frac{\hbar/2\tau}{(\hbar\omega - E_{QD})^2 + (\hbar/2\tau)^2} \quad (6)$$

Where $\hbar/\tau$ expresses the width of the Lorentzian at half its peak value (full width at half maximum, or FWHM). The coupling between the photon and the electron within the QD $\Gamma = \hbar/\tau$. Here the Γ is taken to be 11 meV for demonstration purpose. Combining the equation (3) together with the equations (4) and (6), the analytical expressions for the total emission rates for QD are

$$R_{QD}^{'} = \frac{\Gamma/2}{(\hbar\omega - E_{QD})^2 + (\Gamma/2)^2} f_c(1 - f_v) \tag{7}$$

Where $R_{QD}^{'} = \frac{R_{QD}\hbar}{4\left|M_{h-l}\right|^2 \rho_3^{op}(\hbar\omega)B(\hbar\omega)}$. Here for simplification an assumption of equal number of photons at all wavelengths is taken, i.e. $\rho_3^{op}(\hbar\omega)B(\hbar\omega)$ is a constant. Next, we shall derive the electrochemical potentials for electrons and holes, especially when there are piezoelectric space charges are generated. In order to obtain the chemical potential for electrons or holes, self-consistent approach should be used, by which an initial value of the chemical potential is firstly estimated. Then the below equation is used to calculate the corresponding carrier density [39]

$$n = \frac{1}{2\pi^2}\left(\frac{2m_r}{\hbar^2}\right)^{3/2} \int_{E_{\min}=0}^{E_{\max}=\infty} E^{1/2} \frac{1}{e^{(E-\mu)/k_BT} + 1} dE \tag{8}$$

where the integral has the maximum range of $\mu_{\max} = E_F = \frac{\hbar^2 k_F^2}{2m}$ given by the Fermi energy E_F, $k_F = (3\pi^2 n)^{1/3}$, n is the carrier density. $\mu_{\min}$ can be given using the high temperature limit for a three-dimensional electron gas $\mu_{\min} = k_B T \ln\left(\frac{n}{2}\left(\frac{2\pi\hbar^2}{mk_BT}\right)^{3/2}\right)$. Iterations are conducted numerically according to the above procedure to finally arrive at the correct values for chemical potentials to be used in the equation (7).

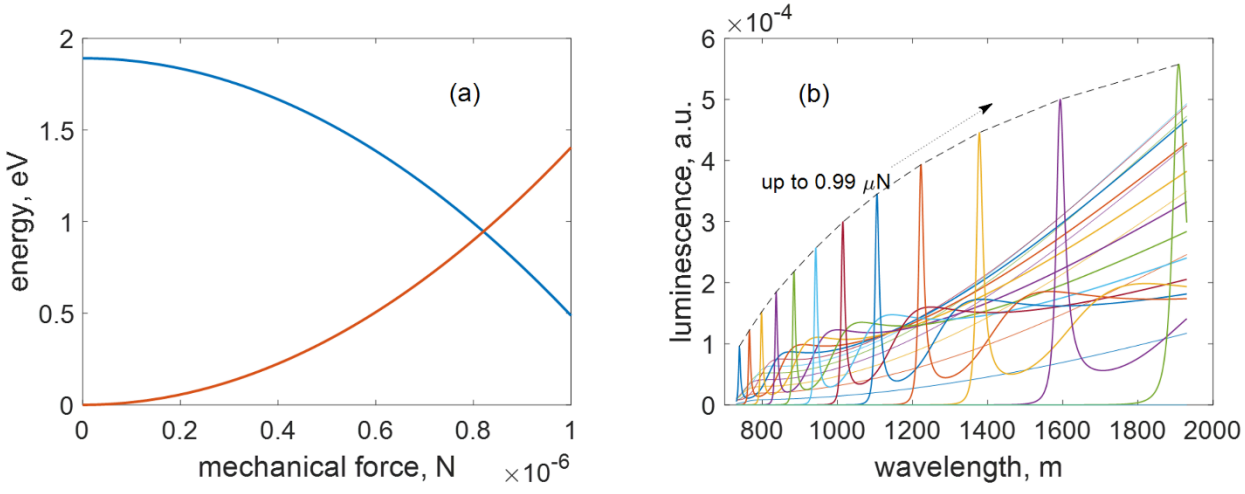

Figure 2, Energy graph of the InN QD under a mechanical force. (a), E_{QD} and E_P vs. mechanical force. (b), Maximum emission intensity over a range of wavelength as increasing the piezoelectric potential. Emission can span from red to infrared.

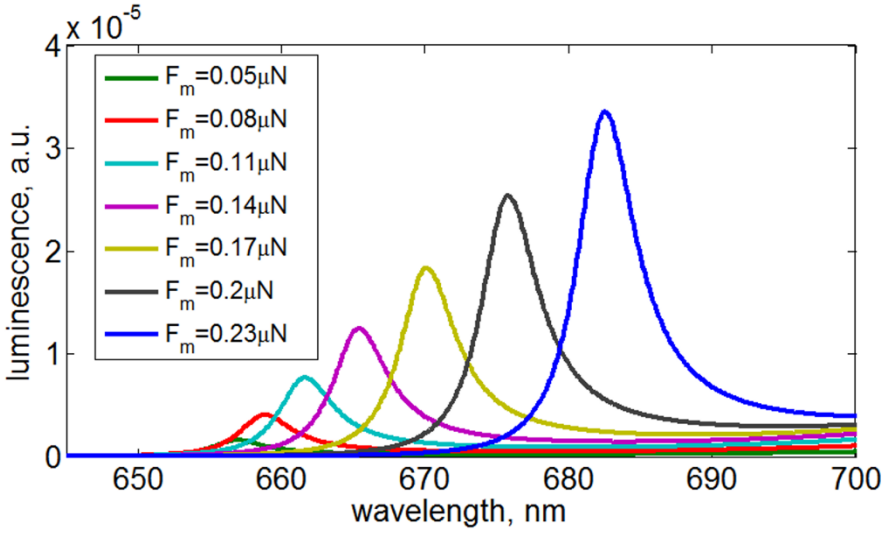

Figure 3, Simulated luminescence over a range of optical wavelength. The mechanical force F_m increases from 0.05 uN to 0.23 uN.

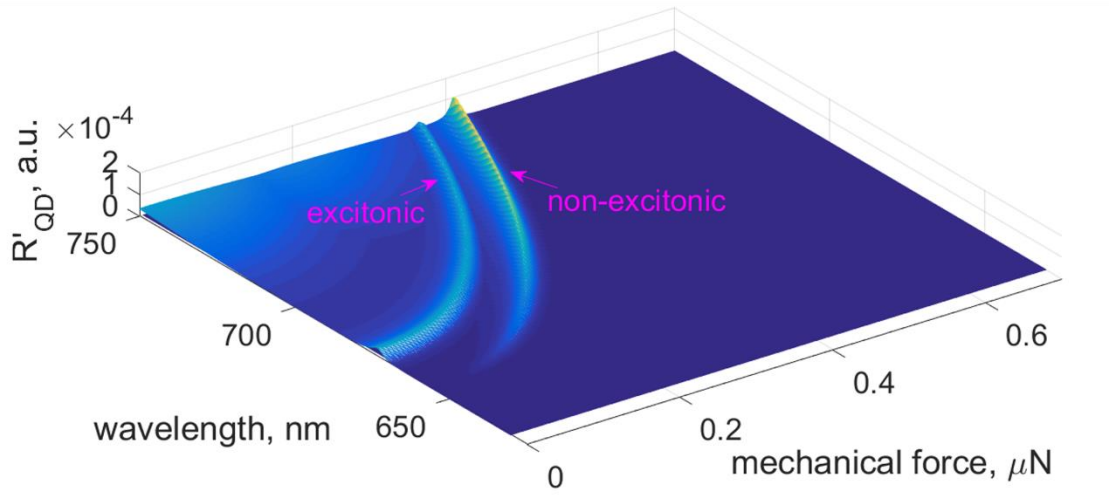

Figure 4, Calculated emission spectrum of InN QD for force varying from 0 to 0.745 uN. Wavelength is swept from 630 nm to 750 nm. When considering excitonic emission at low temperatures, the density of excitons is fixed at 1.68 x 10^{21} m^{-3}.

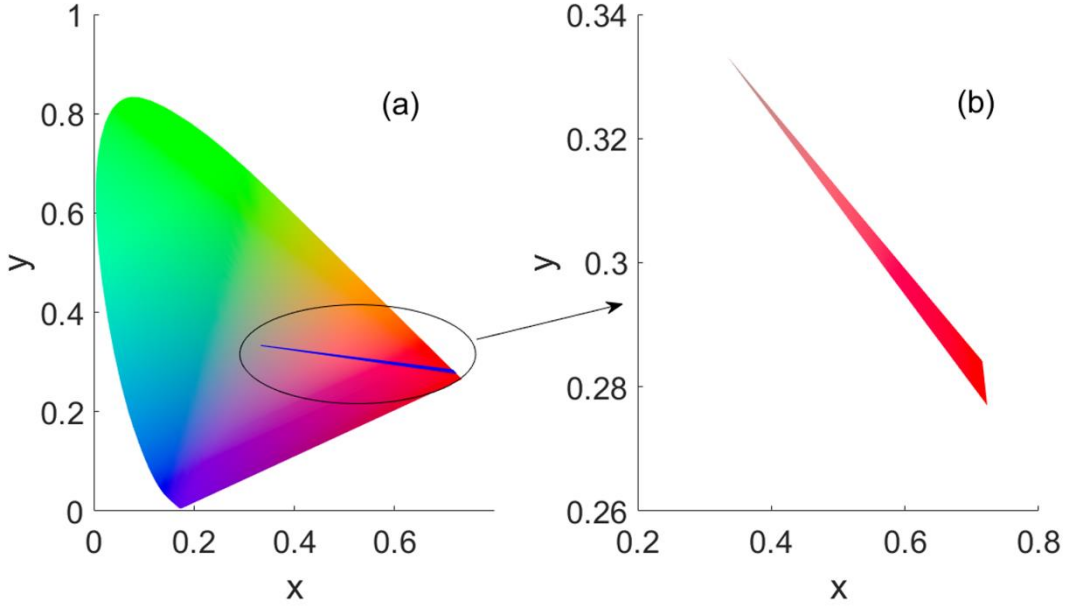

Figure 5, Adjustability of the emission wavelength of the QD by piezotronic effect. (a), intensity spectrum mapped into standard CIE chromaticity diagram. (b) zoomed plot of the intensity spectrum in the chromaticity coordinate.

Results and Discussion

A typical piezoelectric semiconductor QD, the InN cuboidal QD is chosen with the half-length of 50 nm, schematically shown in Figure 1. It is compressed by a mechanical force F_m, and positive charges and negative charges are accumulated at the right and left sides respectively. InN is one of group III nitrides, which are known to have large piezoelectric constants, for example e_{31}=-0.57 C/m^2 for InN, -0.22 and -0.49 C/m^2 for GaN, and -0.58 and -0.6 C/m^2 for AlN. [40] Compared with AlN and GaN, InN has relatively narrow bandgap (1.89 eV in bulk), which is excepted to emit visible red light. In the simulation, effective electron mass is chosen as $0.11m_0$, and effective hole mass is chosen as $0.63m_0$, where m_0 is the single electron mass. Relative dielectric constant of the InN is taken as 15.3, and the piezoelectric constant d_{31} is designated as -1.1 x 10^{-12} C/N. The refractive index n_r is fixed at 3 [41].

For a varied Fm from 0 to 0.5 μN, the piezoelectric potential inducing quantum stark effect is shown in Figure 2, narrowing the bandgap by Ep (Figure 2a). This means that the emission spectrum can be shifted to the infrared regime (630nm – 1800 nm) under the piezoelectric potential. It is also demonstrated that the maximum intensity increases as increasing the mechanical force (Figure 2b).

Further analysis has been performed with regards to the intensity spectrum at each applied mechanical force. The results are displayed in Figure 3, where a clear redshift (emission wavelength increases from around 656nm to 683nm) corresponds to an increasing force (from 0.05 μN to 0.23 μN). As results of increasing number of electrons and holes by the piezotronic effect, the amplitude of the emission has increased.

When the excitonic effect is taken into consideration, further redshift is introduced due to the subtraction of the exciton binding energy. Calculation is conducted for the excitonic emission for the case of the piezoelectric potential is considered. The density of the excitons is fixed at 1.6 x 10^{21} m^{-3}. Figure 4 shows the results of two situations, i.e. excitonic and non-excitonic. For the excitonic luminescence, photons are emitted based on the recombination of excitons. The bandgap in this case is narrower than the non-excitonic emission. Because the excitonic emission dominant at lower temperatures, the non-excitonic emission is important for quantum piezotronic devices at room or higher temperatures applications.

Table I, Comparison of the wavelength tuneability for various semiconductor materials.

	E_g, eV	m_e	m_h	ε_r	d_{31}(pC/N)	n_r	$\delta\lambda/\delta F$ (nm/μN)
CdTe	1.5[42]	0.11[43]	0.89[44]	11[45]	0.19[46]	2.67	50.8
CdSe	1.75[47]	0.12[44]	0.25[48]	5.8[48]	3.92[49]	2.42	1096.7
CdS	2.42[50]	0.21[51]	0.8[51]	5.7[52]	5[53]	2.42	3033
InP	1.35[54]	0.08[55]	0.531[55]	12.5	0.18[56]	3.59	22.8
InAs	0.41[57]	0.026[55]	0.33[55]	15.15	0.65[56]	3.53	760
InN	1.89[58]	0.11[59]	0.63	15.3[60]	1.1	3	167
GaN	3.4[61]	0.13[60]	1.3[62]	8.9[60]	0.9[63]	2.27	213.3

AlN	6.2[61]	0.4[64]	3.52[65]	9.14[66]	1.9[67]	1.99	171.7
GaAs	1.46[68]	0.063	0.51	13[45]	0.68[69]	3.67	108.3

Table II, Wavelength tuneability in terms of pressure, assuming 1 nN is applied.

	δλ/δF **(nm/nN)**	***δλ/δP*** **(nm/MPa)**	**Young's Modulus (GPa)**	**Strain/nN, %**
CdTe	0.05	0.5	52	1.92×10^{-4}
CdSe	1.096	10.96	60	1.67×10^{-4}
CdS	3.033	30.33	45	2.22×10^{-4}
InP	0.023	0.23	61	1.64×10^{-4}
InAs	0.76	7.6	140	7.14×10^{-5}
InN	0.167	1.67	150	6.67×10^{-5}
GaN	0.213	2.13	204	4.90×10^{-5}
AlN	0.171	1.71	320	3.13×10^{-5}
GaAs	0.112	1.12	82.7	1.21×10^{-4}

Figure 5 shows the luminescence in the chromaticity coordinate. Intensity spectrum distribution of the Figure 3 has been mapped into the standard CIE chromaticity diagram. It is seen that adjustability of the QD luminescence can be achieved using the piezotronic effect. For InN QD case, the emission is mainly in the red region. Further increasing the piezoelectric potential, infrared emission can be generated attributed to stronger quantum confined stark effect.

The piezotronic effect on QDs creates a new type of quantum piezotronic devices, which can adjust the luminescence of the QD in terms of both spectrum and intensity. The wavelength of the emission can be adjusted by the piezoelectric potential, for the case of InN QD, the wavelength of the emission increases from around 650 nm to around 1800 nm subjecting to a force up to 1 μN. The intensity of the emission can also be adjusted by the piezoelectric charges.

Furthermore, we investigate the tuneability of the emission wavelength subjecting to the external applied force for various piezoelectric semiconductor QDs. Nine typical piezoelectric semiconductor materials in II-VI, II-V, and III-V categories have been studied, which are popular in designing quantum dos and all have a direct bandgap. Their electronic properties were used in the calculations, such as bandgap E_g, effective mass (electron m_e and hole m_h,), relative permittivity ε_r, piezoelectric constant d_{31} (note for some materials only e_{31} is available, and d_{31} has been derived using $d_{31} = e_{31} / Y$, where Y is the elastic modulus of the material). It is also worth to state that the effective heavy hole mass was used in the analysis. The calculation only considered the first set of resonant peaks. The results (shown in Table I) reveal that the wavelength tuneability of CdS, CdSe, and InAs are 1-2 orders of magnitude higher than the rest materials, which predominantly owes to electronic properties such as large piezoelectric constant and smaller relative dielectric constant.

Further analysis shown in Table II summarizes the relations of the wavelength tuneability, stress, and strain. It is assumed 1 nN force is exerted on the surface of the dot, inducing 100 kPa. The sensitivity in terms of stress is listed in the third column, which is directly proportional to the $\delta\lambda/\delta F$. It is reasonable to conclude that some materials such as CdSe and CdS are better candidates in practical applications, because they are able to detect less than one atmospheric pressure. It is worth mentioning that mechanical strains generated from several nN are very small (~10^{-4} %), which cannot lead to noticeable bandgap variation due to very small change of the atomic structure. Prior experimental study on the strain effect on the CdSe QD suggested that noticeable bandgap changing (such as 47 meV/GPa blueshift, [70] corresponding to approximately 0.017nm/MPa) appears, which is around 1000 times smaller than piezotronic effect shown in the Table II. Another study showed that the bandgap of CdS thin film starts to reduce when the strain is above 1% [71], which is much larger than the strain values due to the piezotronic effect. Previous experimental reports described that a large redshift of the luminescence of GaN quantum wells due to piezotronic effect [63] [72]. It was reported that a pronounced red-shift of the energy gap induced by nanonewton forces for the CdSe/CdS tetrapods [73]. Experiments showed that there is around 0.005 nm/MPa redshift of the CdSe-CdS nanocrystal [74]. Measurement of sub nanometre wavelength change is achievable using interferometer, as established experiment demonstrated 0.001 nm resolution in the 500-nm band and 0.01nm in the 1550-nm band [75]. Piezoelectric potential alters the luminescence of the QD under pressure or force. So we can only consider the piezoelectric d_{31} component of the piezoelectric coefficient under a uniaxial compressive force. A uniaxial tensile force will lead to similar results due to the amplitude of the piezoelectric potential is the same as the case of under a compressive force. For a biaxial force, piezoelectric potential will be calculated using piezoelectric coefficients matrix of different QDs. This paper proposes the idea of controlling luminescence spectrum by piezotronic effect. Effect of carrier density and surface depletion of the piezoelectric potential will be considered

in our future works. Piezotronic effects on the 1D nanowires are reported in the following references [76] [72] [77] [78]. The device concept can be applied as pressure sensors, which will be coated on any small-scale features such as cells and miniaturised devices. To implement the concept, possible fabrication procedures include printing or spin-coating a layer of pressure sensitive materials e.g. CdSe QDs onto the surface exposed to any external forces. A passivation layer will be normally needed to protect the QDs layer from being delaminated/damaged by any direct-contact forces.

Conclusion

The adjustability of the luminescence of semiconductor quantum dots have been demonstrated through quantum mechanics analysis with the piezotronic effect. For one of group III nitrides materials – InN, the bulk band gap has been substantially tuned by the quantum confined stark effect due to the piezoelectric potential. The emission spectrum can span from red to infrared upon a small mechanical force. Intensity can also be adjusted by the induced piezoelectric charges. For both low temperature and room temperature cases, the emission spectrum can be tuned by the piezoelectric potential. Widely used piezoelectric semiconductor materials for engineering quantum dots have been analysed with regards to the wavelength tuneability. Calculation results show CdS has much higher $\delta\lambda/\delta F$ compared with others.

Acknowledgements

LL appreciates Swansea University and SPARC II project for support, YZ and JN would like to thank University of Electronic Science and Technology of China for support.

References

[1] Dubertret, B.;Skourides, P.;Norris, D. J.;Noireaux, V.;Brivanlou, A. H.; Libchaber, A. In Vivo Imaging of Quantum Dots Encapsulated in Phospholipid Micelles. Science 2002, 298, 1759-1762.

[2] Shao, L.;Gao, Y.; Yan, F. Semiconductor Quantum Dots for Biomedicial Applications. Sensors (Basel, Switzerland) 2011, 11, 11736-11751.

[3] Dhenadhayalan, N.;Lee, H.-L.;Yadav, K.;Lin, K.-C.;Lin, Y.-T.; Chang, A. H. H. Silicon Quantum Dot-Based Fluorescence Turn-On Metal Ion Sensors in Live Cells. ACS Applied Materials & Interfaces 2016, 8, 23953-23962.

[4] Medintz, I. L.;Uyeda, H. T.;Goldman, E. R.; Mattoussi, H. Quantum dot bioconjugates for imaging, labelling and sensing. Nat Mater 2005, 4, 435-446.

[5] Xing, Y.; Rao, J. H. Quantum dot bioconjugates for in vitro diagnostics & in vivo imaging. Cancer Biomark. 2008, 4, 307-319.

[6] Segarra, C.;Climente, J. I.;Polovitsyn, A.;Rajadell, F.;Moreels, I.; Planelles, J. Piezoelectric Control of the Exciton Wave Function in Colloidal CdSe/CdS Nanocrystals. The Journal of Physical Chemistry Letters 2016, 7, 2182-2188.

[7] Christodoulou, S.;Rajadell, F.;Casu, A.;Vaccaro, G.;Grim, J. Q.;Genovese, A.;Manna, L.;Climente, J. I.;Meinardi, F.;Rainò, G.;Stöferle, T.;Mahrt, R. F.;Planelles, J.;Brovelli, S.; Moreels, I. Band structure engineering via piezoelectric fields in strained anisotropic CdSe/CdS nanocrystals. Nature Communications 2015, 6, 7905.

[8] Conley, H. J.;Wang, B.;Ziegler, J. I.;Haglund, R. F.;Pantelides, S. T.; Bolotin, K. I. Bandgap Engineering of Strained Monolayer and Bilayer MoS2. Nano Lett. 2013, 13, 3626-3630.

[9] Lu, P.;Wu, X.;Guo, W.; Zeng, X. C. Strain-dependent electronic and magnetic properties of MoS2 monolayer, bilayer, nanoribbons and nanotubes. Physical Chemistry Chemical Physics 2012, 14, 13035-13040.

[10] Simmonds, P. J.;Yerino, C. D.;Sun, M.;Liang, B.;Huffaker, D. L.;Dorogan, V. G.;Mazur, Y.;Salamo, G.; Lee, M. L. Tuning Quantum Dot Luminescence Below the Bulk Band Gap Using Tensile Strain. ACS Nano 2013, 7, 5017-5023.

[11] Germanis, S.;Katsidis, C.;Tsintzos, S.;Stavrinidis, A.;Konstantinidis, G.;Florini, N.;Kioseoglou, J.;Dimitrakopulos, G. P.;Kehagias, T.;Hatzopoulos, Z.; Pelekanos, N. T. Enhanced Stark Tuning of Single InAs $(211)B$ Quantum Dots due to Nonlinear Piezoelectric Effect in Zincblende Nanostructures. Physical Review Applied 2016, 6, 014004.

[12] Kuhl, U.;Izrailev, F. M.;Krokhin, A. A.; Stöckmann, H.-J. Experimental observation of the mobility edge in a waveguide with correlated disorder. Applied Physics Letters 2000, 77, 633-635.

[13] Florini, N.;Dimitrakopulos, G. P.;Kioseoglou, J.;Germanis, S.;Katsidis, C.;Hatzopoulos, Z.;Pelekanos, N. T.; Kehagias, T. Structure, strain, and composition profiling of InAs/GaAs(211)B quantum dot superlattices. Journal of Applied Physics 2016, 119, 034304.

[14] Tetsuya, T.;Shigetoshi, S.;Maki, K.;Miho, K.;Hideo, T.;Hiroshi, A.; Isamu, A. Quantum-Confined Stark Effect due to Piezoelectric Fields in GaInN Strained Quantum Wells. Japanese Journal of Applied Physics 1997, 36, L382.

[15] Peng, X. G.;Manna, L.;Yang, W. D.;Wickham, J.;Scher, E.;Kadavanich, A.; Alivisatos, A. P. Shape control of CdSe nanocrystals. Nature 2000, 404, 59-61.

[16] Vahala, K. J. Optical microcavities. Nature 2003, 424, 839-846.

[17] Hu, J. T.;Li, L. S.;Yang, W. D.;Manna, L.;Wang, L. W.; Alivisatos, A. P. Linearly polarized emission from colloidal semiconductor quantum rods. Science 2001, 292, 2060-2063.

[18] Yoffe, A. D. Semiconductor quantum dots and related systems: electronic, optical, luminescence and related properties of low dimensional systems. Adv. Phys. 2001, 50, 1-208.

[19] de Assis, P. L.;Yeo, I.;Gloppe, A.;Nguyen, H. A.;Tumanov, D.;Dupont-Ferrier, E.;Malik, N. S.;Dupuy, E.;Claudon, J.;Gerard, J. M.;Auffeves, A.;Arcizet, O.;Richard, M.; Poizat, J. P. Strain-Gradient Position Mapping of Semiconductor Quantum Dots. Phys. Rev. Lett. 2017, 118.

[20] Corsini, N. R. C.;Hine, N. D. M.;Haynes, P. D.; Molteni, C. Unravelling the Roles of Size, Ligands, and Pressure in the Piezochromic Properties of CdS Nanocrystals. Nano Lett. 2017, 17, 1042-1048.

[21] Okazaki, Y.;Mahboob, I.;Onomitsu, K.;Sasaki, S.; Yamaguchi, H. Gate-controlled electromechanical backaction induced by a quantum dot. Nat. Commun. 2016, 7.

[22] Chen, Y.;Zhang, J. X.;Zopf, M.;Jung, K. B.;Zhang, Y.;Keil, R.;Ding, F.; Schmidt, O. G. Wavelength-tunable entangled photons from silicon-integrated III-V quantum dots. Nat. Commun. 2016, 7.

[23] Wang, X. F.;Yu, R. M.;Peng, W. B.;Wu, W. Z.;Li, S. T.; Wang, Z. L. Temperature Dependence of the Piezotronic and Piezophototronic Effects in a-axis GaN Nanobelts. Advanced Materials 2015, 27, 8067-8074.

[24] Wang, Z. L. Piezotronic and Piezophototronic Effects. Journal of Physical Chemistry Letters 2010, 1, 1388-1393.

[25] Wen, X. N.;Wu, W. Z.;Pan, C. F.;Hu, Y. F.;Yang, Q.; Wang, Z. L. Development and progress in piezotronics. Nano Energy 2015, 14, 276-295.

[26] Zhou, J.;Gu, Y. D.;Fei, P.;Mai, W. J.;Gao, Y. F.;Yang, R. S.;Bao, G.; Wang, Z. L. Flexible piezotronic strain sensor. Nano Lett. 2008, 8, 3035-3040.

[27] Wu, W. Z.;Wei, Y. G.; Wang, Z. L. Strain-Gated Piezotronic Logic Nanodevices. Advanced Materials 2010, 22, 4711-+.

[28] Zhang, Y.;Liu, Y.; Wang, Z. L. Fundamental Theory of Piezotronics. Advanced Materials 2011, 23, 3004-3013.

[29] Wu, W. Z.;Wen, X. N.; Wang, Z. L. Taxel-Addressable Matrix of Vertical-Nanowire Piezotronic Transistors for Active and Adaptive Tactile Imaging. Science 2013, 340, 952-957.

[30] Wu, W. Z.;Wang, L.;Li, Y. L.;Zhang, F.;Lin, L.;Niu, S. M.;Chenet, D.;Zhang, X.;Hao, Y. F.;Heinz, T. F.;Hone, J.; Wang, Z. L. Piezoelectricity of single-atomic-layer MoS2 for energy conversion and piezotronics. Nature 2014, 514, 470-+.

[31] Zhang, Y.; Li, L. Piezophototronic effect enhanced luminescence of zinc oxide nanowires. Nano Energy 2016, 22, 533-538.

[32] Chen, Y.;Zhang, Y.;Karnaushenko, D.;Chen, L.;Hao, J.;Ding, F.; Schmidt, O. G. Addressable and Color-Tunable Piezophotonic Light-Emitting Stripes. Advanced Materials 2017, 29, n/a-n/a.

[33] Wong, M.-C.;Chen, L.;Tsang, M.-K.;Zhang, Y.; Hao, J. Magnetic-Induced Luminescence from Flexible Composite Laminates by Coupling Magnetic Field to Piezophotonic Effect. Advanced Materials 2015, 27, 4488-4495.

[34] Bai, G.;Tsang, M.-K.; Hao, J. Luminescent Ions in Advanced Composite Materials for Multifunctional Applications. Advanced Functional Materials 2016, 26, 6330-6350.

[35] Fox, M. Optical Properties of Solids; Oxford University Press: London, 2001.

[36] Renard, J.;Songmuang, R.;Tourbot, G.;Bougerol, C.;Daudin, B.; Gayral, B. Evidence for quantum-confined Stark effect in GaN/AlN quantum dots in nanowires. Physical Review B 2009, 80.

[37] Zhang, M.;Bhattacharya, P.; Guo, W. InGaN/GaN self-organized quantum dot green light emitting diodes with reduced efficiency droop. Applied Physics Letters 2010, 97, 011103.

[38] Singh, J. Appendix A: Fermi Golden Rule. In Modern Physics for Engineers. Wiley-VCH Verlag GmbH, 2007; pp 347-352.

[39] Sze, S. M.; Ng, K. K. Physics of Semiconductor Devices; John Wiley & Sons, 2006.

[40] Takeuchi, T.;Wetzel, C.;Yamaguchi, S.;Sakai, H.;Amano, H.;Akasaki, I.;Kaneko, Y.;Nakagawa, S.;Yamaoka, Y.; Yamada, N. Determination of piezoelectric fields in strained GaInN quantum wells using the quantum-confined Stark effect. Applied Physics Letters 1998, 73, 1691-1693.

[41] Piprek, J. Nitride Semiconductor Devices: Principles and Simulation; Wiley, 2007.

[42] Fonthal, G.;Tirado-Mejía, L.;Marín-Hurtado, J. I.;Ariza-Calderón, H.; Mendoza-Alvarez, J. G. Temperature dependence of the band gap energy of crystalline CdTe. Journal of Physics and Chemistry of Solids 2000, 61, 579-583.

[43] Marple, D. T. F. Effective Electron Mass in CdTe. Physical Review 1963, 129, 2466-2470.

[44] Rubio Ponce, A.;Olguín, D.; Hernández Calderón, I. Calculation of the effective masses of II-VI semiconductor compounds Superficies y vacío 2003, 16, 26-28.

[45] Strzalkowski, I.;Joshi, S.; Crowell, C. R. Dielectric constant and its temperature dependence for GaAs, CdTe, and ZnSe. Applied Physics Letters 1976, 28, 350-352.

[46] Bernardini, F.;Fiorentini, V.; Vanderbilt, D. Spontaneous polarization and piezoelectric constants of III-V nitrides. Physical Review B 1997, 56, R10024-R10027.

[47] Dai, Q.;Song, Y.;Li, D.;Chen, H.;Kan, S.;Zou, B.;Wang, Y.;Deng, Y.;Hou, Y.;Yu, S.;Chen, L.;Liu, B.; Zou, G. Temperature dependence of band gap in CdSe nanocrystals. Chemical Physics Letters 2007, 439, 65-68.

[48] Wakaoka, T.;Hirai, K.;Murayama, K.;Takano, Y.;Takagi, H.;Furukawa, S.; Kitagawa, S. Confined synthesis of CdSe quantum dots in the pores of metal-organic frameworks. Journal of Materials Chemistry C 2014, 2, 7173-7175.

[49] Bowen, C. R.;Topolov, V. Y.; Kim, H. A. Modern Piezoelectric Energy-Harvesting Materials; Springer Series in Materials Science, 2016.

[50] Oliva, A. I.;Solı;amp;x;s-Canto, O.;Castro, R.;guez, R.; Quintana, P. Formation of the band gap energy on CdS thin films growth by two different techniques. Thin Solid Films 2001, 391, 28-35.

[51] Winkelmann, K.;Noviello, T.; Brooks, S. Preparation of CdS Nanoparticles by First-Year Undergraduates. Journal of Chemical Education 2007, 84, 709.

[52] Lippens, P. E.; Lannoo, M. Calculation of the band gap for small CdS and ZnS crystallites. Physical Review B 1989, 39, 10935-10942.

[53] Shvydka, D.;Drayton, J.;Compaan, A. D.; Karpov, V. G. Piezo-effect and physics of CdS-based thin-film photovoltaics. Applied Physics Letters 2005, 87, 123505.

[54] Pavesi, L.;Piazza, F.;Rudra, A.;Carlin, J. F.; Ilegems, M. Temperature dependence of the InP band gap from a photoluminescence study. Physical Review B 1991, 44, 9052-9055.

[55] Kim, Y.-S.;Hummer, K.; Kresse, G. Accurate band structures and effective masses for InP, InAs, and InSb using hybrid functionals. Physical Review B 2009, 80, 035203.

[56] Hajlaoui, C.;Pedesseau, L.;Raouafi, F.;Ben Cheikh Larbi, F.;Even, J.; Jancu, J.-M. Ab initio calculations of polarization, piezoelectric constants, and elastic constants of InAs and InP in the wurtzite phase. Journal of Experimental and Theoretical Physics 2015, 121, 246-249.

[57] Svensson, S. P.;Sarney, W. L.;Hier, H.;Lin, Y.;Wang, D.;Donetsky, D.;Shterengas, L.;Kipshidze, G.; Belenky, G. Band gap of InAs${}_{1\ensuremath{-}x}$Sb${}_{x}$ with native lattice constant. Physical Review B 2012, 86, 245205.

[58] Tansley, T. L.; Foley, C. P. Optical band gap of indium nitride. Journal of Applied Physics 1986, 59, 3241-3244.

[59] Lambrecht, W. R. L.; Segall, B. Anomalous band-gap behavior and phase stability of c-BN\char21{}diamond alloys. Physical Review B 1993, 47, 9289-9296.

[60] Levinshtein M.E.;Rumyantsev S.L.; Shur M.S. Properties of Advanced SemiconductorMaterials GaN, AlN, InN, BN, SiC, SiGe John Wiley & Sons, Inc.: New York, 2001.

[61] Strite, S.; Morkoç, H. GaN, AlN, and InN: A review. Journal of Vacuum Science & Technology B: Microelectronics and Nanometer Structures Processing, Measurement, and Phenomena 1992, 10, 1237-1266.

[62] Martin, G.;Botchkarev, A.;Rockett, A.; Morkoç, H. Valence-band discontinuities of wurtzite GaN, AlN, and InN heterojunctions measured by x-ray photoemission spectroscopy. Applied Physics Letters 1996, 68, 2541-2543.

[63] Seo Im, J.;Kollmer, H.;Off, J.;Sohmer, A.;Scholz, F.; Hangleiter, A. Reduction of oscillator strength due to piezoelectric fields in ${\mathrm{G}\mathrm{a}\mathrm{N}/\mathrm{A}\mathrm{l}}_{x}{\mathrm{Ga}}_{1\ensuremath{-}x}\mathrm{N}$ quantum wells. Physical Review B 1998, 57, R9435-R9438.

[64] Xu, Y.-N.; Ching, W. Y. Electronic, optical, and structural properties of some wurtzite crystals. Physical Review B 1993, 48, 4335-4351.

[65] Suzuki, M.; Uenoyama, T. Strain effect on electronic and optical properties of GaN/AlGaN quantum-well lasers. Journal of Applied Physics 1996, 80, 6868-6874.

[66] Collins, A. T.;Lightowlers, E. C.; Dean, P. J. Lattice Vibration Spectra of Aluminum Nitride. Physical Review 1967, 158, 833-838.

[67] Sinha, N.;Wabiszewski, G. E.;Mahameed, R.;Felmetsger, V. V.;Tanner, S. M.;Carpick, R. W.; Piazza, G. Piezoelectric aluminum nitride nanoelectromechanical actuators. Applied Physics Letters 2009, 95, 053106.

[68] Kusch, P.;Breuer, S.;Ramsteiner, M.;Geelhaar, L.;Riechert, H.; Reich, S. Band gap of wurtzite GaAs: A resonant Raman study. Physical Review B 2012, 86, 075317.

[69] Fricke, K. Piezoelectric properties of GaAs for application in stress transducers. Journal of Applied Physics 1991, 70, 914-918.

[70] Reparaz, J. S.;Goñi, A. R.;Alonso, M. I.;Perez-Paz, M. N.; Tamargo, M. C. Size-dependent strain effects in self-assembled CdSe quantum dots with Zn0.38Cd0.23Mg0.39Se barriers. Applied Physics Letters 2006, 89, 231109.

[71] Liwei, S.;Yun, Q.;Jing, H.;Yifeng, D.;Licheng, Q.;Ling, W.; Gang, T. Strain-assisted structural transformation and band gap tuning in BeO, MgTe, CdS and 2H-SiC: A hybrid density functional study. EPL (Europhysics Letters) 2014, 106, 57001.

[72] Wang, X.;Peng, W.;Pan, C.; Wang, Z. L. Piezotronics and piezo-phototronics based on a -axis nano/microwires: fundamentals and applications. Semiconductor Science and Technology 2017, 32, 043005.

[73] Choi, C. L.;Koski, K. J.;Sivasankar, S.; Alivisatos, A. P. Strain-Dependent Photoluminescence Behavior of CdSe/CdS Nanocrystals with Spherical, Linear, and Branched Topologies. Nano Letters 2009, 9, 3544-3549.

[74] Choi, C. L.;Koski, K. J.;Olson, A. C. K.; Alivisatos, A. P. Luminescent nanocrystal stress gauge. Proceedings of the National Academy of Sciences 2010, 107, 21306-21310.

[75] Mikami, A.;Irisawa, A.; Watanabe, Y. High-resolution optical spectrum measurements using an interferometer. In Conference Proceedings. 10th Anniversary. IMTC/94. Advanced Technologies in I & M. 1994 IEEE Instrumentation and Measurement Technolgy Conference (Cat. No.94CH3424-9), 1994; pp 1499-1500 vol.1493.

[76] Wei, B.;Zheng, K.;Ji, Y.;Zhang, Y.;Zhang, Z.; Han, X. Size-Dependent Bandgap Modulation of ZnO Nanowires by Tensile Strain. Nano Letters 2012, 12, 4595-4599.

[77] Lu, S.;Qi, J.;Gu, Y.;Liu, S.;Xu, Q.;Wang, Z.;Liang, Q.; Zhang, Y. Influence of the carrier concentration on the piezotronic effect in a ZnO/Au Schottky junction. Nanoscale 2015, 7, 4461-4467.

[78] Hu, G.;Zhou, R.;Yu, R.;Dong, L.;Pan, C.; Wang, Z. L. Piezotronic effect enhanced Schottky-contact ZnO micro/nanowire humidity sensors. Nano Research 2014, 7, 1083-1091.